NATIONAL UNIVERSITY OF SCIENCE AND TECHNOLOGY POLITEHNICA OF BUCHAREST

Faculty of APPLIED SCIENCE

ABSTRACT

DOCTORAL THESIS

Simulations of Ultra-High Intensity Laser Pulse Interaction with Solid Targets

AUTHOR:

DRD. BUDRIGĂ (MARTIŞ) MARIA

DOCTORAL COMMISSION

President	prof. dr. Cristina STAN, Director of the Doctoral School	from	UNST Politehnica of Bucharest S.D.S.A.
Thesis coordinator	Prof. dr. Gheorghe CĂTA-DANIL	from	UNST Politehnica of Bucharest
Member	Prof. dr. Alexandru JIPA	from	University of Bucharest, Faculty of Physics
Member	Prof. dr. Ionel LAZANU	from	University of Bucharest, Faculty of Physics
Member	Prof. dr. Emil PETRESCU	from	UNST Politehnica of Bucharest

Bucharest

2023

CONTENTS

INTRODUCTION

Article acceleration is essential in many areas of research, contributing substantially to the development of many aspects of human life. Among the remarkable advances in science and technology that have been possible due to particle accelerators are: treating cancer more efficiently than traditional methods, semiconductor manufacturing and discovery of new energy sources. accelerators are also the basis for scientific research at famous centers such as C.E.R.N. where in 2013 the Higgs boson was discovered.

Unlike classic accelerators, particle accelerators with high power lasers are much small in size and particle acceleration (electron, ion) is made over a distance of centimeter order up to 100 m.

Ultra-high intensity laser pulses offer the ability to accelerate particles to energies from hundreds of MeV to a few GeV. Accelerators can be designed to produce collisions of two types: with a fixed target (a particle of a fixed target) is struck and with beams (two particle beams collide coming from opposite directions).

Also in recent decades, a lot of target geometries have been proposed to obtain very energetic protons. Some works have shown that the interaction of an ultra-high intensity laser pulses with a micro-con target can generate protons accelerated to tens of MeV energies with a low divergence angle and high laser absorption. An experiment at the Vulcan feature demonstrates that the interaction of an ultra-high intensity laser pulses with a very thin foil can generate accelerated protons at energies exceeding 94 MeV energies.

In Romania, the processing of laser materials is much inclined towards micro- and nano-processing, especially technologies for depositing thin films, and the technology that is used to create the nanotints that i will describe in my thesis is polymerization with two photons**.**

The issues addressed in this field of research require the use of plasma. It can be said that in this type of environment, the predominant processes are kinetic and collective in nature, there are many nonlinear phenomena. This makes it difficult to use analytical models, so that Particle-In-Cell codes have become important in modeling parameters and optimizing experimental work.

The codes based on the Particle-In-Cell method used in the numerical modeling of the laser-plasma interaction are based on solving electromagnetic fields using Maxwell equations coupled with Vlasov equations.

Chapter 1

NOTIONS FOR THE PLASMA PHYSICS, LASERS AND ULTRA-HIGH INTENSITY LASER PULSE INTERACTION WITH PLASMA

In the first subchapter I present notions of plasma physics. The Vlasov equation which together with the Maxwell equations allow us to calculate the load and current density. Because when an intense laser pulse passes through the plasma, the ponderomotive force acts to expel particles from the regions with the highest laser intensity occurs, we described this force further. The second subchapter contains notions of high power laser physics.. Because in the simulations I used the Gaussian pulses, I further described their parameters. PIC codes use dimensionless units because the numerical calculation time is reduced and therefore for the calculation of the intensity we used the dimension amplitude of the electric field, a_0,. In the case of ultra-short pulses, they describe the principle of Chirped Pulse Amplification and laser components. The last 2 subchapters contain information on accelerating electrically charged particles. In the third part I will describe the acceleration of the electrons by the wake field generated by an ultra-intense laser field, and in the latter part the acceleration of ions as a result of the interaction of ultra-intense plasma laser fields. Here we have described the mechanisms for accelerating Target Normal Acceleration of Sheath (TNSA), Collisionless Shock Acceleration (CSA), Coulumbian Explosions and Radiation Pressure Acceleration (RPA).

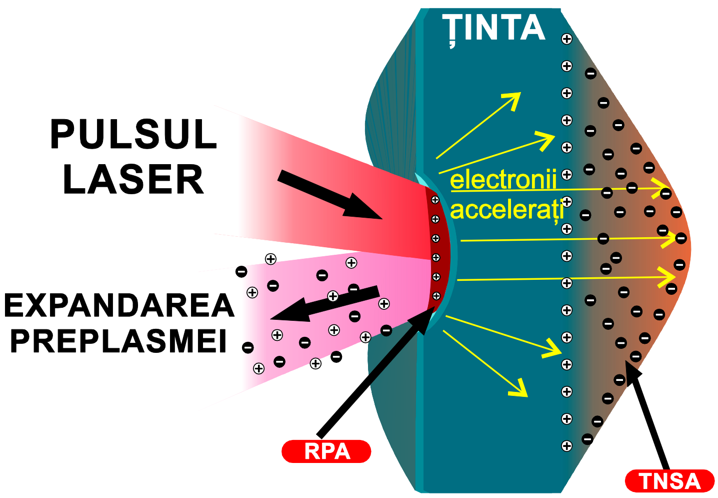

Fig.1 Particle acceleration mechanisms

Chapter 2

PARTICLE-IN-CELL SIMULATIONS (PIC). SMILE CODE

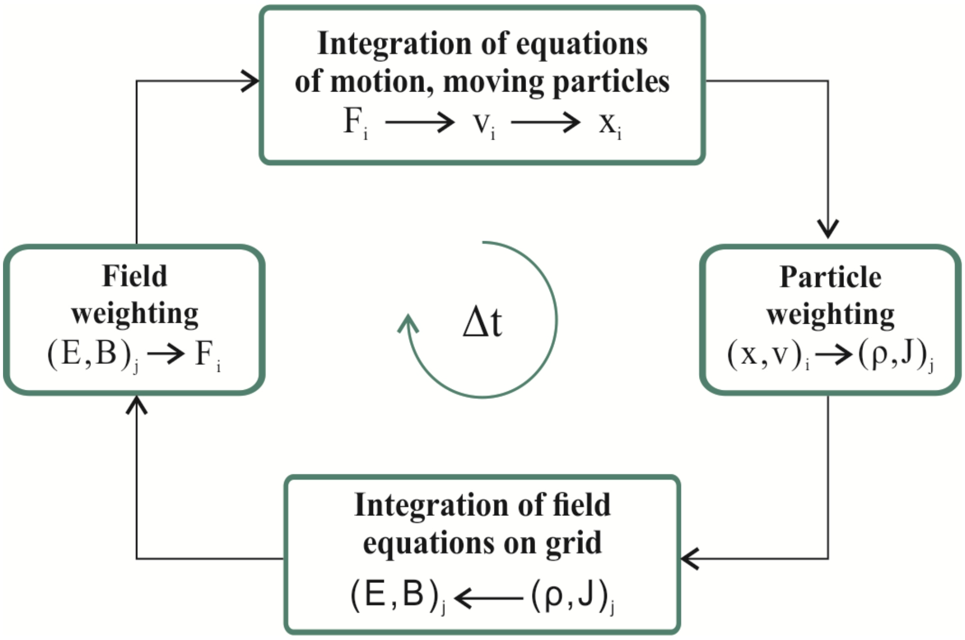

Fig. 2 A Particle-in Cell cycle one step away from the simulation algorithm

The name of the SMILE Code comes from the first letters of the words **S**imulation **M**atter **I**rradiated by **L**ight at **E**xtreme **I**ntensities. Smile is a PIC simulation code, open source, object-oriented.. It was developed in a collaborative framework, including physicists and high-performance computing experts (HPC).

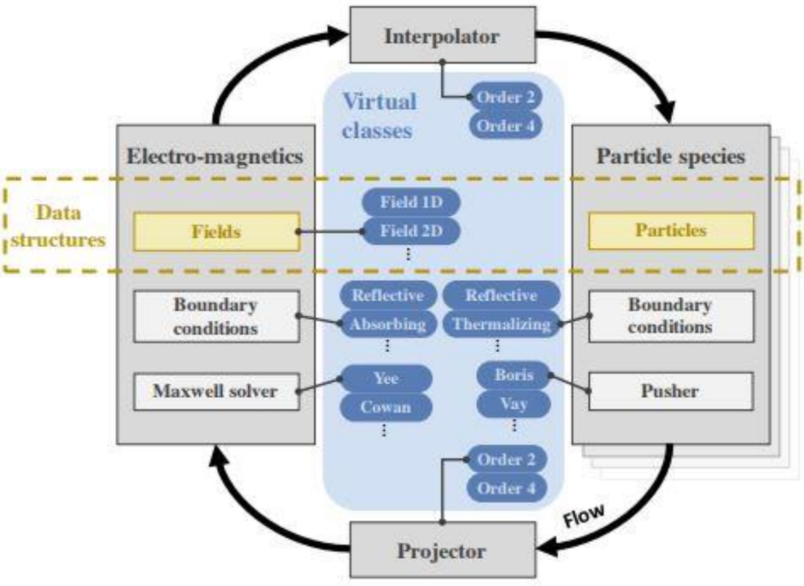

Fig. 3 C++ flow, data classes and structure in Smile

Chapter 3

PROTON AND ION ACCELERATION OF AN ULTRA-HIGH INTENSITY LASER PULSE WITH NANOSTRUCTURED FLAT-TOP CONE TARGETS

We studied the interaction of an ultra-high intensity laser pulse with two new types of microtargets, using PIC simulations and simulations based on the FDTD method.

The first target is a plastic microcon with a flat nanostructured foil on top, tens of nanometers thick. I used this in the thesis as " nanostructured flat-top cone". The second target is a plastic microcon, with a top foil composed of two nano-layers. The first nanostrat is a nano-layer foil with a thickness of tens of nanometers on which a second nanostrat consisting of plastic nanospheres, identical in size, with the same diameter of tens of nanometers, tangent to each other and tangent to the tip of the cone. We called this second target „cone with nanospheres".

The laser beam always comes from the left. The thickness of the cone walls is *4 μm* and the height is *20 μm* for both targets.

Because I set out to find out what is the optimal diameter of nanosphere to get very energetic protons and carbon ions, we extracted from the literature the range of optimal values in which it is located and performed the simulation for the interaction of an ultra-intense laser pulse with a ultra-thin flat plastic foil. Thus, we obtained that the maximum energy of the protons is obtained for the thickness of the foil of 80 nm.

For the target „ cone with nanospheres " we kept constant the thickness of the first layer, which is a foil, of *40 nm*, and I varied the diameter of the nanospheres from *20 nm* to *80 nm*, with steps of *20 nm*.

For the nanostructured flat-top cone target, we considered the thickness of the top foil as the sum of the diameter of the nanosphere of the top of the " cone with nanospheres" and *40 nm*. Thus, the thickness of the foil at the top of the nanostructured flat-top cone varies in the range from *60 nm* to *120 nm*, with steps of *20 n*m. A *0.5 μm* preplasma is considered on the walls of the cone.

The 2 targets were inserted into a two-dimensional simulation box, measuring 60 μm × 75 μm. This simulation box is related to a system of orthogonal axes with the Ox and Oy axes.

A cell in the PIC simulation has a size of *10 nm* × *10 nm*. Because the simulated plasma and preplasma are completely ionized, we introduced into a cell 21 electrons, 3 protons and 3 carbon ions C^{6+}.The total simulation time is 230 fs and the time step is 0.033 fs.

In all the simulations I used linearly polarized and circularly polarized ultra-intense lasers pulses. Ultra-intense pulse parameters in the simulations and laser beam intensity values have values such as those of the ELI-NP lasers. The linearly polarized laser pulse has an intensity of $2{,}16 \times 10^{22} W cm^{-2}$ and the circularly polarized laser pulse has an intensity of 2 times higher than that of the linear laser pulse polarized, mean $4{,}32 \times 10^{22} W cm^{-2}$.

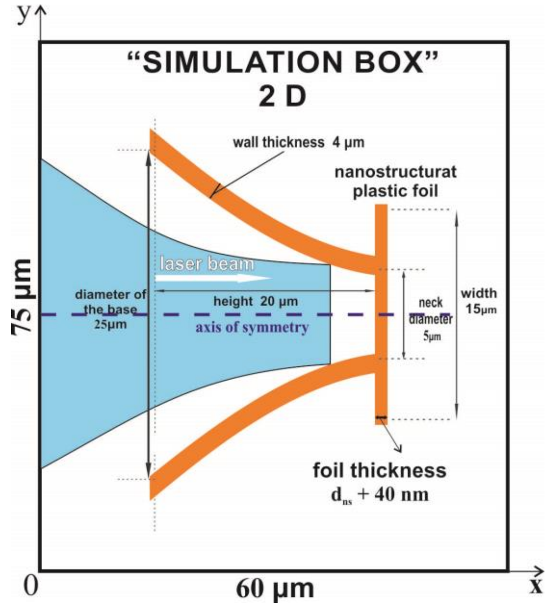

Fig. 4 Nanostructured flat-top cone

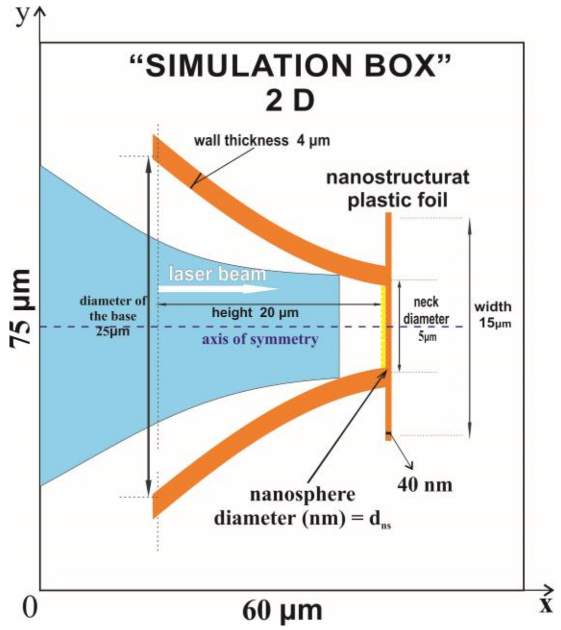

Fig. 5 Cone with nanospheres

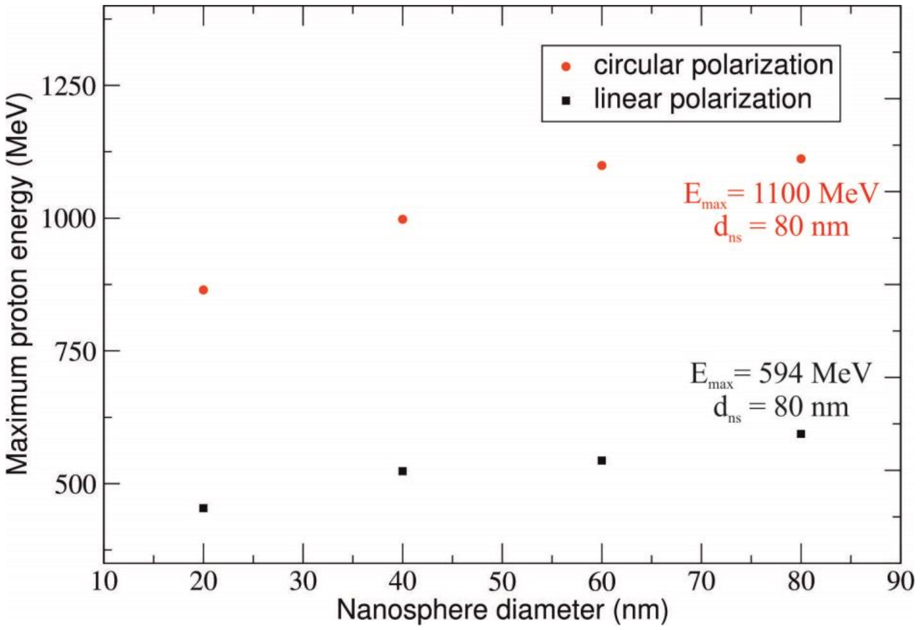

Fig. 6 Dependence of maximum proton energy from the diameter of nanosphere

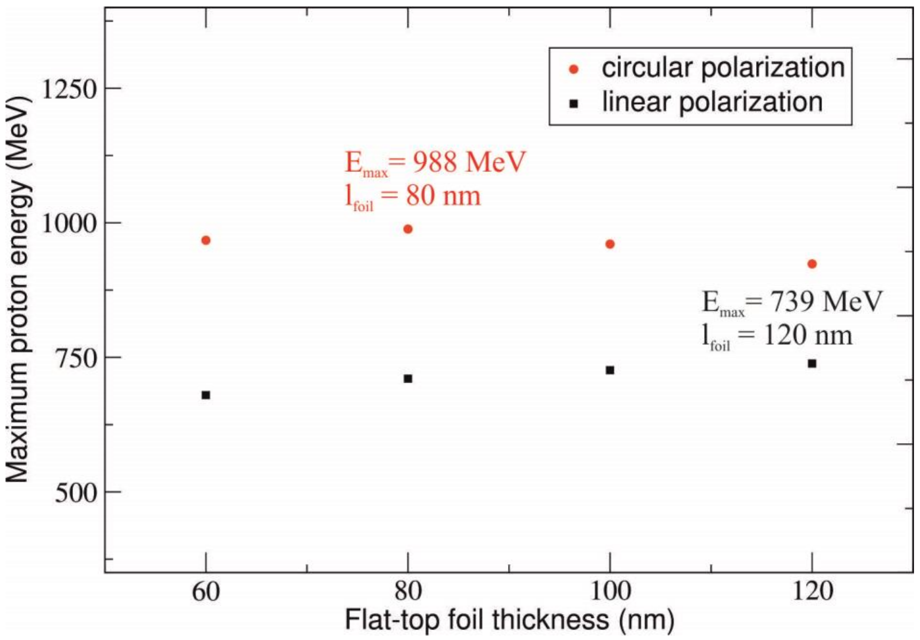

Fig. 7 Dependence of the maximum energy of the protons on the thickness of the top foil

We obtained that optimal target for obtaining very energetic protons :

- circulary polarized laser pulse is Cone with nanospheres with a nanosphere diameter of 80 nm, maximum energy E_{max} = 1,1 GeV
- linearly polarized laser pulse is the nanostructured flat-top cone with the foil thickness of 120 nm, maximum energy E_{max} = 988 MeV

Next we studied the behavior of the longitudinal component of the $E_x$electric field for both polarizations of the laser pulse at the simulation time 168 fs, for the time step 63 τ_0, in cases of *20 nm*, *40 nm*, *60 nm* and *80 nm* nanosphere diameters..

.

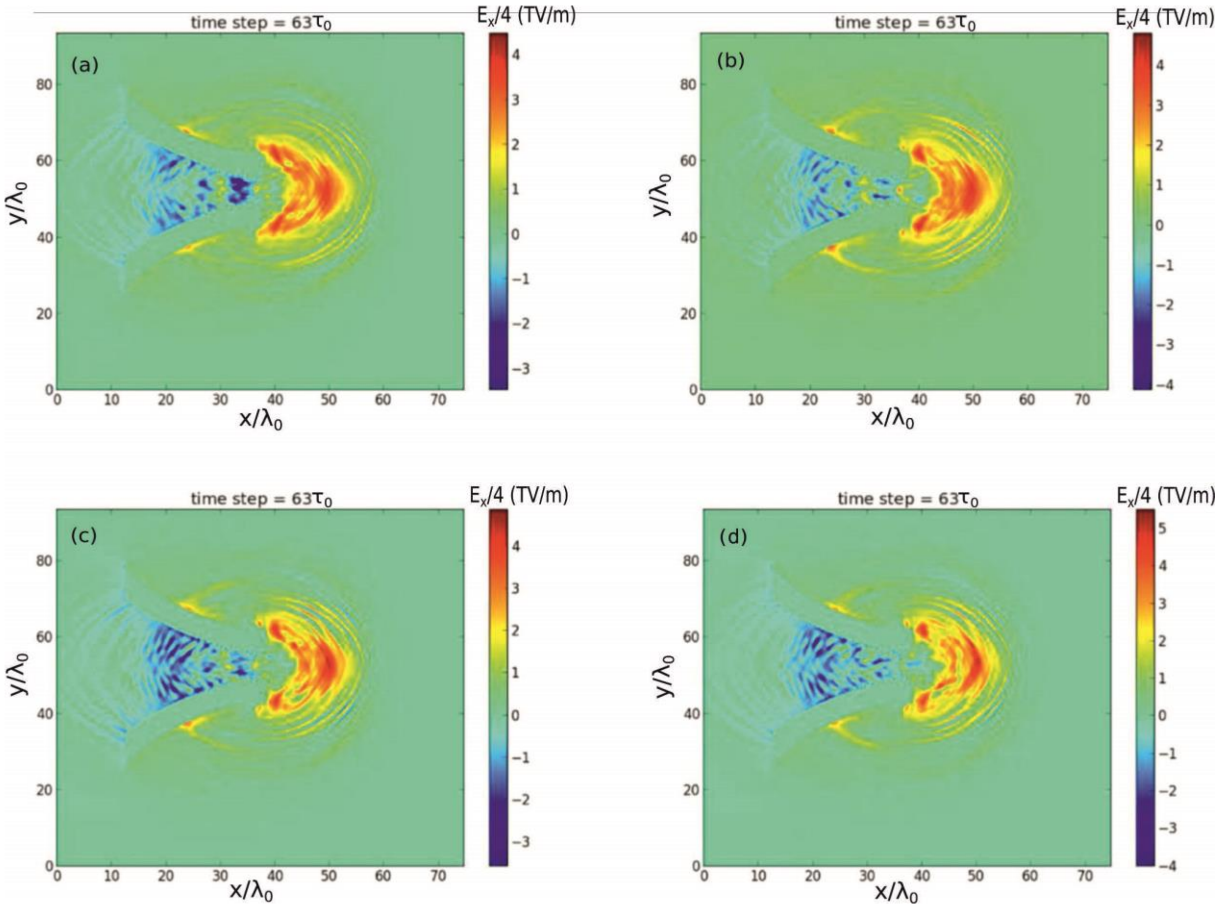

Fig. 8 Distribution of the longitudinal component of the electric field

We obtained that the maximum value of the E_x increases directly proportional to the diameter of the nanosphere.

Proton energy spectra for a cone target at the interaction of a linear and circular polarized ultraintens laser pulse at simulation time *t = 240 fs* for *x ≥ 30 μm* were further studied.

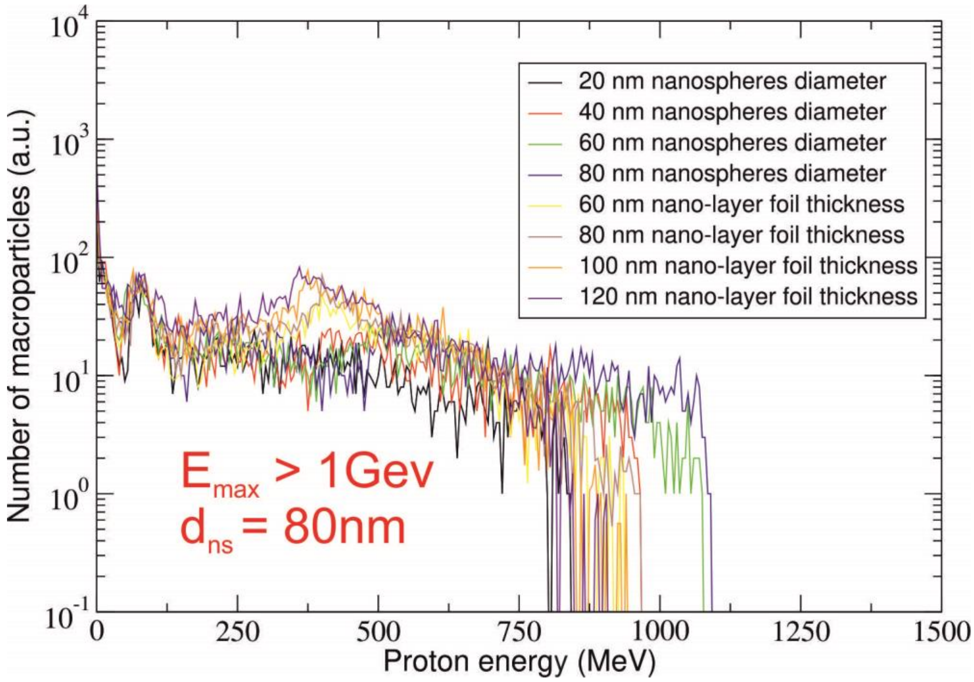

Fig. 9 Energy distribution of protons. Circularly polarized laser pulse.

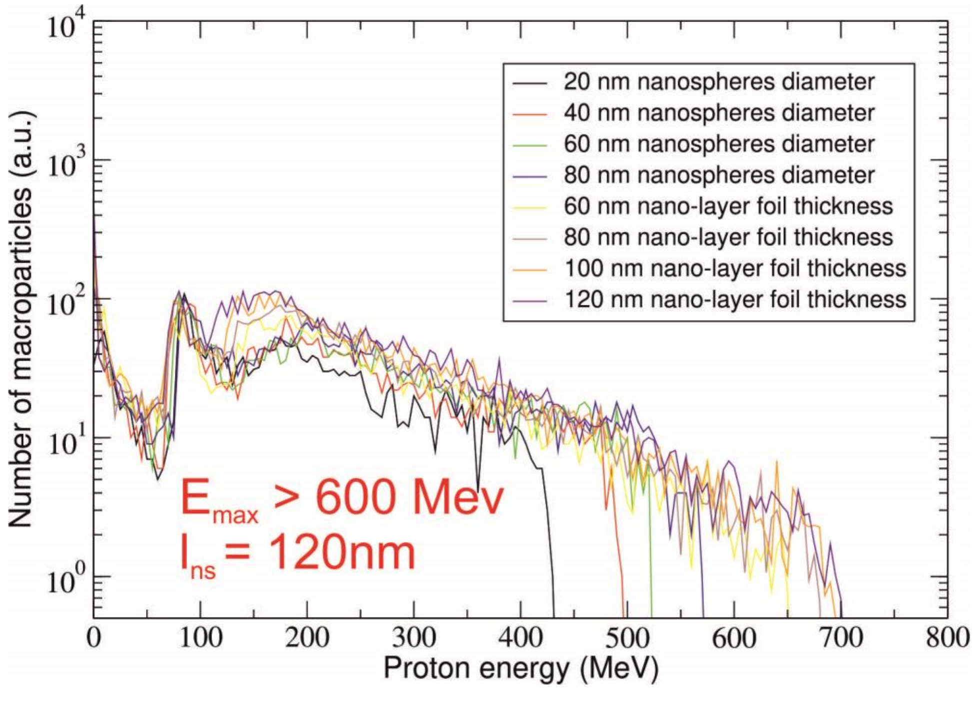

Fig. 10 Energy distribution of protons. Linearly polarized laser pulse

We obtained that the maximum number of energy protons for the circulary polarized laser pulse is the cone with nanospheres, nanosphere diameter of *80 nm* with E_{max} > 1GeV, and for the linearly polarized laser pulse is the nanostructured flat-top cone with a foil thickness of *120 nm* with E_{max} > 600 MeV.

We studied the angular distribution of protons for the cone with nanospheres and nanostructured flat-top cone. The ultraintens laser pulse is linear and circular polarized. The simulation time is $t = 240\ fs$ for protons with $35{,}2\ \mu m \leq y \leq 40\ \mu m,\ 52\mu m \leq x \leq 60\ \mu m$ (circulary polarized laser pulse) and $48\ \mu m \leq x \leq 56\ \mu m$ (linearly polarized laser pulse). We considered protons with energies greater than *600 MeV* for CP laser pulse and greater than *300 MeV* for LP laser pulse.

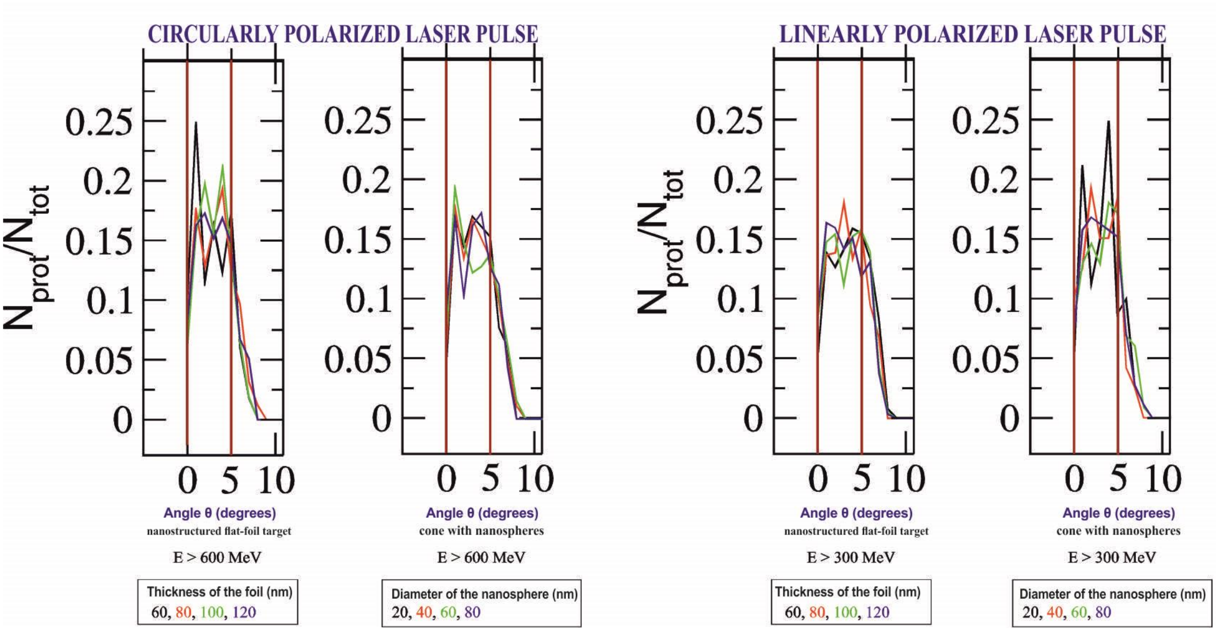

Fig. 11 Angular distribution of protons for cone with nanospheres and nanostructured flat-top cone

We obtained that the low angular divergence ($\theta \in (0°,\ 5°)$) implies increased efficiency of the interaction process.

Because ultra-high intensity laser pulse interaction with targets that are made of plastic, carbon ions are obtained, in the second part of Chapter 3 we studied the acceleration of carbon C^{6+}. We also studied the dependence of the maximum energy of carbon ions on the thickness of the top foil for the nanostructured flat-top cone and on the diameter nanospheres of the cone with nanospheres for the linearly and circularly polarized laser pulse.

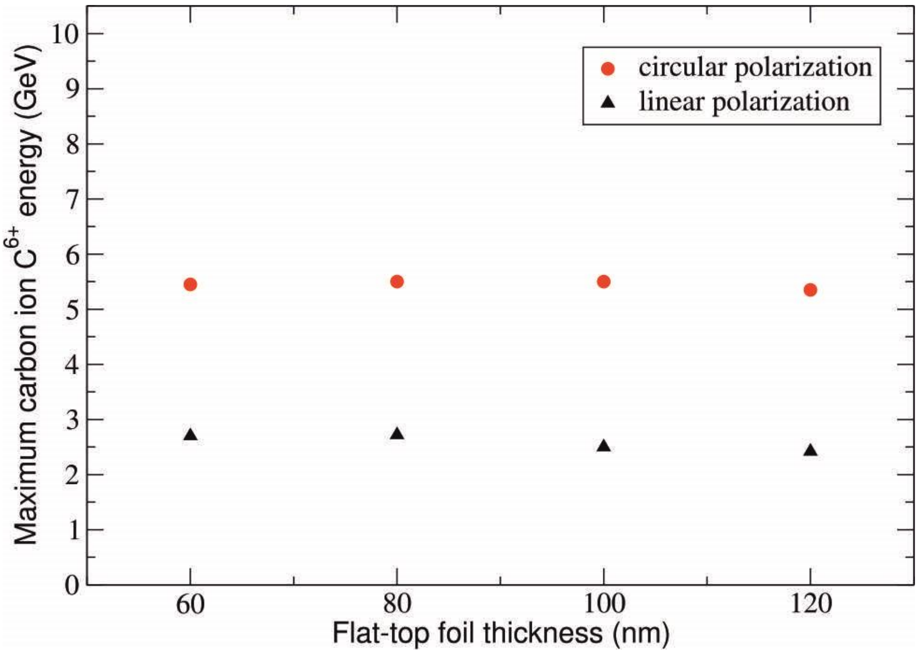

Fig.12 Dependence of the maximum energy of carbon ions of the thickness of the top foil

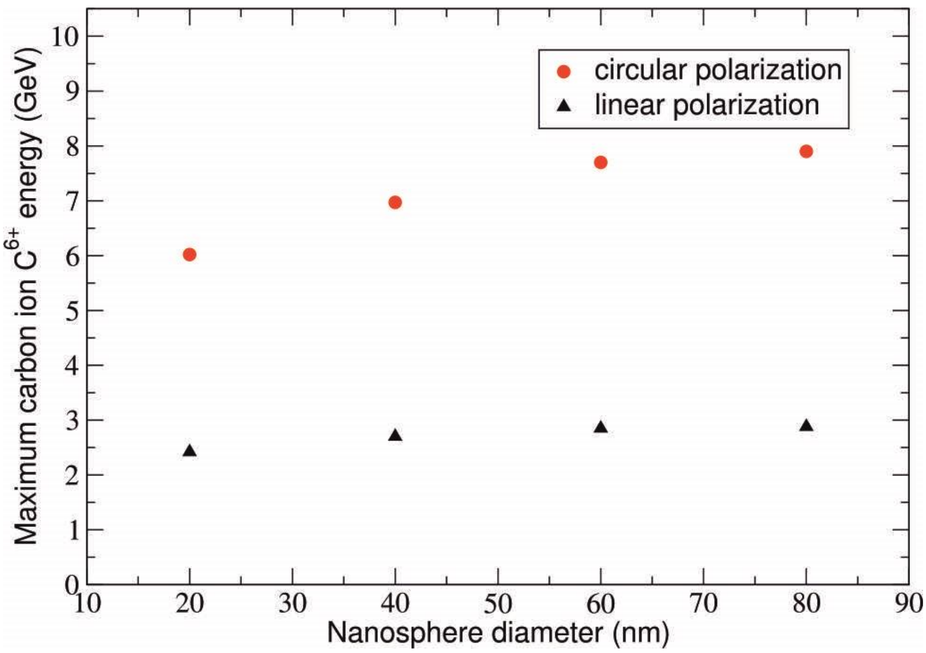

Fig.13 Dependence of maximum energy of carbon ions on the diameter of nanospheres

We obtained that for the nanostructured flat-top cone E_{max} is inversely proportional to the thickness of the top foil and for the cone with nanospheres, E_{max} is directly proportional to the diameter of the nanosphere.

Next I present the energy spectra of the carbon ions for a nanostructured flat-top cone at the interaction of a linearly and circulary polarized ultraintense laser pulse at the simulation time *t = 240 fs*, for $x \geq 30\ \mu m$.

The third subchapter " TNSA combined with RPA ", because from the introduction of the RPA regime of ultraintens laser pulse ion acceleration to the interaction with a foil target a lot of works have been dedicated to the study of this ion-laser acceleration regime. A hybrid regime that includes TNSA and RPA has been introduced and used to explain the acceleration of ions in quasi-monoenergetic beams by an ultraintens LP laser pulse that interacts with a foil target.

In this subchapter we have shown that protons are accelerated by a hybrid acceleration mechanism, including TNSA and RPA for a LP and CP ultra-high intensity laser pulse which interacting with a cone with nanospheres. We only presented the results for a cone with nanospheres with a of 80 nm diameter and nanostructured flat-top cone with a thickness of the top foil *40 nm* and a circulary polarized laser pulse. We studied the evolution of the distribution of carbon protons and ions for 2 steps of time: $67\tau_0$ and $78\tau_0$. At step $67\tau_0$ I present the graphs at the simulation time *t = 178 fs* and at step $78\tau_0$ respectively at the simulation time *t = 208 fs* for protons and ions of carbon. Next we represented the proton phase space at simulation times of *138 fs*, *160 fs* and *178 fs* for both polarizations of the laser pulse.

We simulated the maximum variation of the proton energy depending on the simulation time starting from *t = 100 fs* and ending at *t = 250 fs*, for linearly and circulary polarized laser pulse.

We compared the results for the longitudinal component of the electric field $E_x$obtained by the FDTD method and by the PIC method . The same qualitative results were obtained by PIC simulations where the highest proton energy is obtained for the nanosphere diameter equal to *80 nm* for both LP and CP laser pulses.

Chapter 4

PROTON AND ION ACCELERATION OF AN ULTRA-HIGH INTENSITY LASER PULSE WITH AN ULTRA-THIN NANOSTRUCTURED FLAT-FOIL TARGET

These flat targets of tens of nanometers, which differ from targets that have been studied by other authors of hundreds of nanometers. The research we did differs from previous studies by using an linearly and circulary polarized ultra-high intensity laser pulse. Because the target is a 2-layer nanostructured flat foil: the first layer is made of plastic nanospheres, tangent to each other and tangent to the second layer which is a flat plastic foil, the nanosphere will have a diameter of tens of nanometers and have an advantage of this approach which comes from the low cost of nanosphere production.

In this chapter, the parameters of the ultra-intense pulses in the simulations and the values of the laser beam intensities have values such as those used in ELI-NP. The total simulation time is *190 fs* for the linearly polarized laser pulse and *180 fs* for the circulary polarized laser puls. The time step is *0.022 fs*.

The target was inserted into a two-dimensional simulation box measuring $40\ \mu m \times 40\ \mu m$. This simulation box is related to a system of orthogonal Ox and Oy axes.

A cell in the PIC simulation has a *6.7 nm × 6.7 nm* size. Because the simulated plasma and preplasma are completely ionized, we introduced into a cell 21 electrons, 3 protons and 3 carbon ions C^{6+}. The total simulation time is *230 fs* and the time step is 0.033 fs. A $0.5\ \mu m$ preplasma is considered on the walls of the cone. The laser beam comes from the left and the waist of the laser beam is $9.52\ \mu m$.

Several authors obtained the optimal thickness of the nanostructured flat foil in the range 70 – 100 nm and as I pointed out above, in the Chapter 2, we performed the simulation for the interaction of an ultra-high intensity laser pulse with a ultra-thin nanostructured foil target, where we obtained that the maximum proton energy for the film thickness of *80 nm*. Thus, we kept constant the total thickness of the nanostructured foil at 80 nm, this being the sum between the diameter of the nanosphere and the thickness of the flat foil. We varied the diameter of the nanospheres from *0 nm* to *80 nm*, with steps of *10 nm*, and the flat foil from *80 nm* to *0 nm*, with steps of *10 nm*.

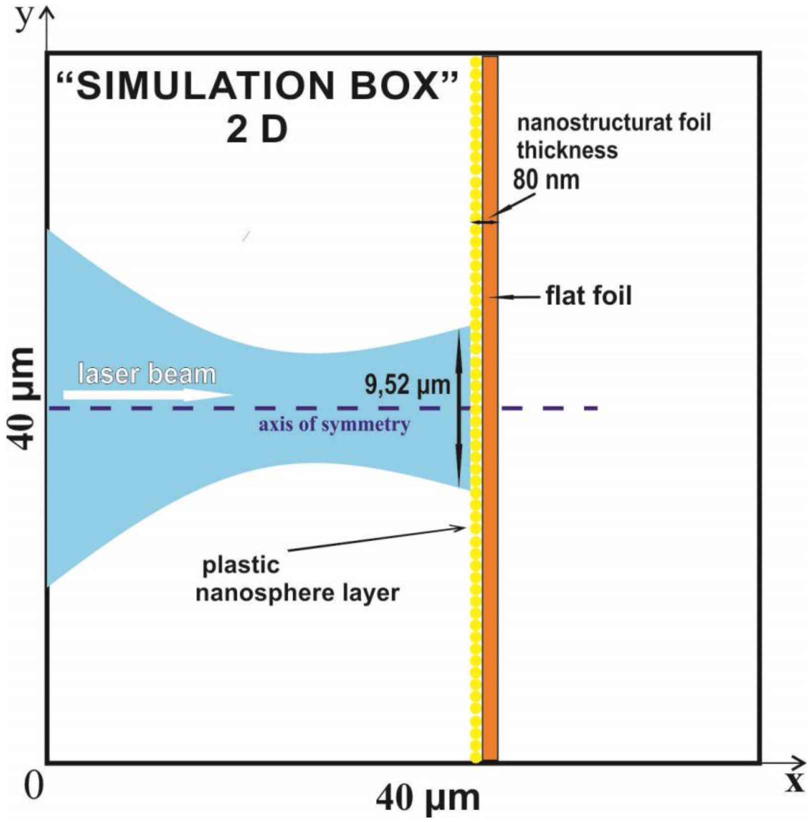

Fig. 14 Geometry of ultra-thin nanostructured flat-foil target

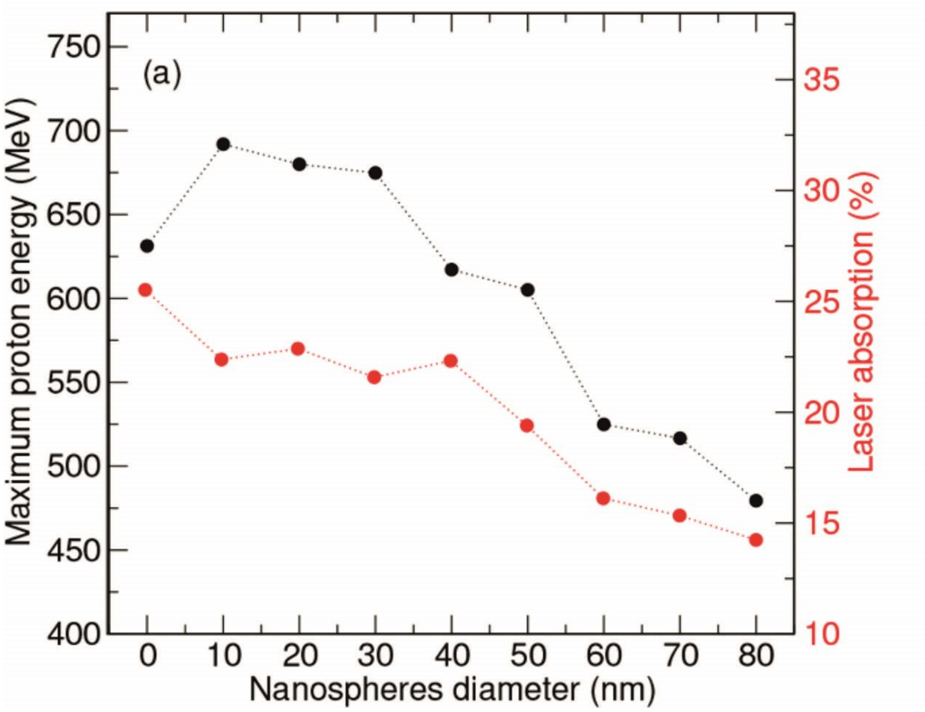

Fig. 15 (a) Maximum proton energy (black points) and laser absorption (red points) as a function of the nanospheres diameter. The ultra-high intensity laser pulse is liniar polarized..

In the case of circularly polarized laser pulse we obtain that maximum energy is 1,21 GeV and for the nanosphere diameter = *40 nm.*

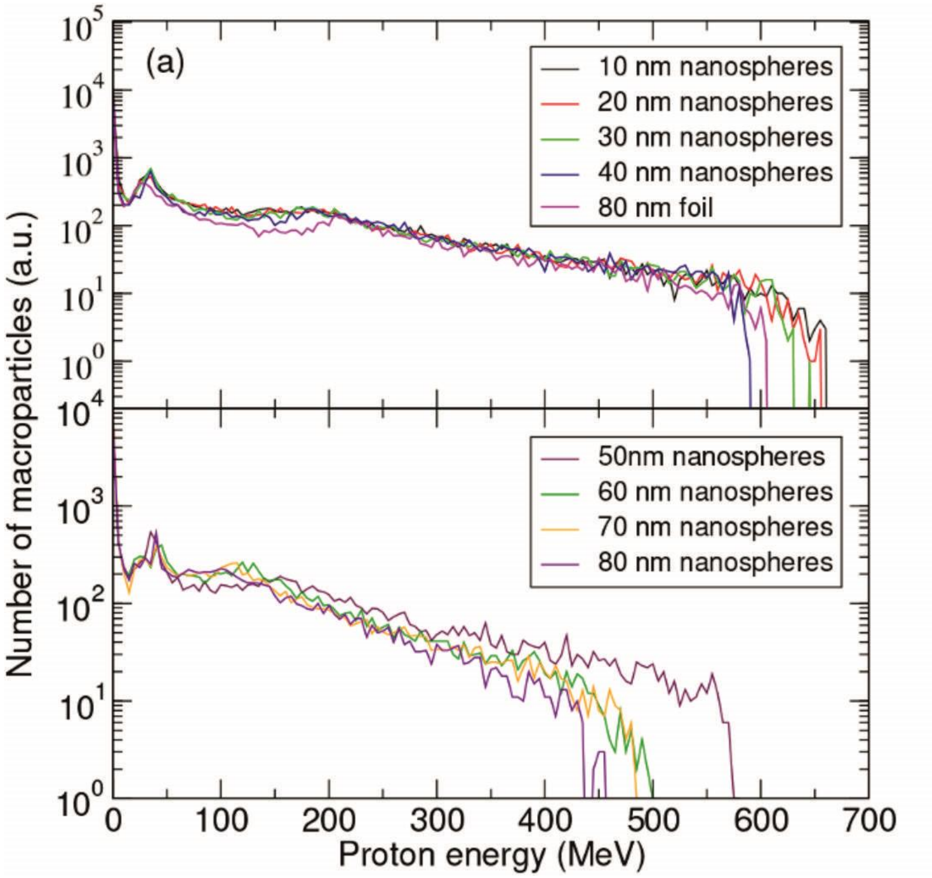

Fig. 16 Energy distribution of protons, circularly polarized laser pulse

Next we studied the behavior of the longitudinal component E_x of the electric field depending on time, from *0 fs* to *150 fs* with *17.6 μm* ≤ *y* ≤ *24.8 μm.*

I described the energy spectrum and angular distribution of protons at simulation time *t = 173 fs* for protons with energies greater than *300 MeV*

I got that for low angular divergence at $\theta = 2^{\circ}$ we have increased efficiency of the interaction process (*E* > *300 MeV*) for flat foil with thickness 80nm,

We notice that the optimal diameter of the nanosphere for the highest number of protons accelerated with low angular divergence is *30 nm*.

For the circulary polarized laser pulsewe studied the dependence from the diameter of the nanosphere of the maximum energy of the protons and the laser absorption. Next we studied the behavior of the longitudinal components E_x and transveral E_y of the electric field as a function of time, from *0 fs* to *150 fs*. In the case of the polarized circular laser pulse we have that maximum E_y > maximum E_x, for each diameter of the nanosphere.

Here we also studied the maximum amplitude of the electric field $E = \sqrt{E_x^2 + E_y^2}$ as a function of time.

We also studied the angular distribution of protons at the simulation time *t = 173 fs* for protons with $17.6\mu m \leq y \leq 24.8\ \mu m$. We considered protons with energies greater than 600 MeV.

I still have " Proton Accceleration regime: RPA and TNSA " where I considered linearly and circulary polarized laser pulse.

In the case of a linearly polarized laser pulse and for a target consisting of a layer of nanosphere with a diameter of *30 nm* on a flat foil with a thickness of 50 nm, simulated proton distribution with energies greater than 300 MeV at 2 simulation times: *112 fs* and *173 fs* and proton phase space $(x, (\beta\gamma)_x)$, at simulation times *45 fs*, *67 fs* and *80 fs* after the interaction of the laser pulse with the nanostructured foil. We also studied the distribution of maximum proton energy over time.

In the case of a circulary polarized laser pulse and for a target consisting of a layer of nanosphere with a diameter of *60 nm* on a flat foil with a thickness of *20 nm*, we studied the evolution of the distribution of protons and carbon ions for 2 steps of time: $55\tau_0$ și $60\tau_0$. At step $55\tau_0$ present the graphs at the simulation time t = 146 fs, and at the time step $60\tau_0$ respectively I present the graphs at the simulation time *t = 160 fs*, for protons and carbon ions. Next we represented the proton phase space at simulation times of *48 fs*, *56 fs* and *61 fs*.

We also researched the maximum variation of proton energy depending on the simulation time starting from *t = 40 fs* to *t = 180 fs*, for linearly and circulary polarized laser pulse.

In the second part of chapter 4 we studied *" Acceleration of carbon ions C^{6+}"* using PIC simulations. Due to the ultra-high intensity of the laser pulse interacting with a nanostructured plastic foil (CH), the plasma contains carbon ion C^{6+}. We represented the dependence of the maximum energy of the carbon ion C^{6+} per nucleon depending on the diameter of the nanospheres for a linearly and circulary polarized ultra-high intensity laser pulse.

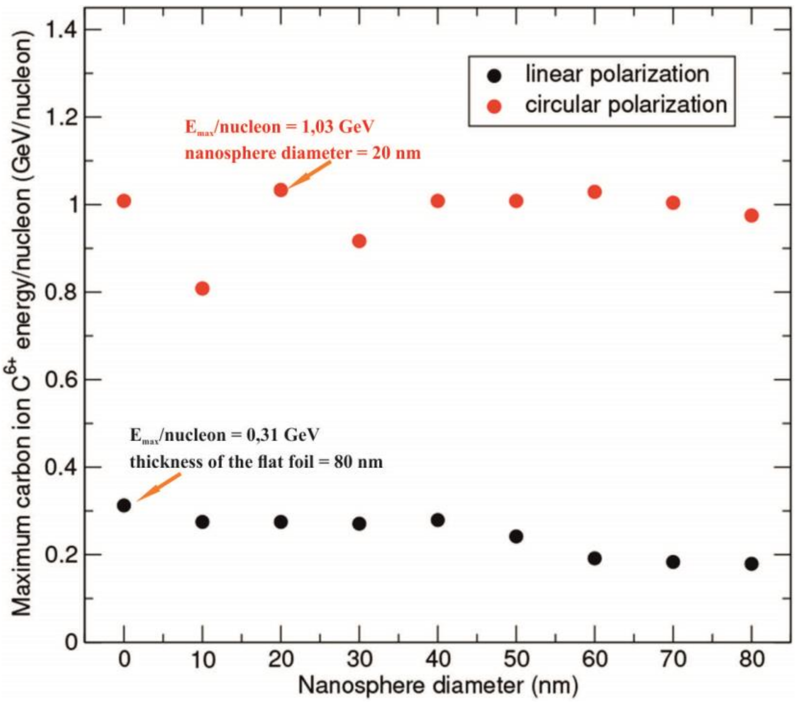

Fig. 17 Maximum energy dependence of carbon ion on the diameter of nanospheres

We obtained that $\mathrm{E_{max}}$ /nucleon for the LP laser pulse is 0.31 GeV / nucleon for a flat-foil with a thickness of *80 nm* and for the CP laser pulse, is 1.03 GeV / nucleon for a nanostructured flat-foil with a nanosphere diameter of *20 nm*.

Then describe the energy spectrum of ions at the simulation time t = 173 fs depending on the diameter of the nanospheres for the linearly and circulary polarized laser pulse.

We got that the maximum number of energy ions is obtained for linearly polarized laser pulse in the case of the flat- foil with a thickness of 80 nm.

Carbon ion phase space C^{6+}, $(x, (\beta\gamma)_x)$, is simulated after the interaction of the linearly polarized laser pulse with nanostructured foil with a nanosphere diameter of 30 nm and a foil thickness of 50 nm at times 45 fs, 67 fs and 80 fs and for the circular laser pulse at times 48 fs, 56 fs and 61 fs.

The third subchapter " *Evolution of the electromagnetic field by the FDTD*" is a complementary study of the interaction of an ultraintens laser pulse with a nanostructured foil target was performed in order to isolate geometric parameters that influence the laser-plasma interaction. The FDTD numerical study uses the same geometries and interaction parameters as those that were chosen in PIC simulations and involves a Gaussian laser source that initially propagates along the x-axis, to the point of interaction of the ultraintens laser pulse with the target of a nanostructured plastic flat foil. The laser source has a diameter of *5,6 μm* and is positioned at a distance of *10 μm* from the point of interaction along the propagation axis x. The thickness of the layer consisting of foil and nanosphere is maintained at *80 nm*.

The thickness of the foil is in the range 0 and 70 nm with steps of 10 nm in a complementary way to the variation of the diameter of the nanosphere between 10 and 80 nm. The intensity of the electromagnetic field is researched both for the linearly and circularly laser pulse, at a given moment, when the maximum field is reached.

In FDTD simulations we represented the evolution of the longitudinal component of the electric field, E_x measured at the point of interaction of the ultraintens LP and CP pulse with a flat and nanostructured plastic foil depending on the diameter of the nanoprobes.

We compared these E_x results obtained by FDTD simulations with those obtained from PIC simulations.

From the graphs obtained here for both polarized pulses and nanosphere diameters between 0 nm and 80 nm there is a sudden decrease in E_x from nanostructured flat-foil with a nanosphere diameter of 30 nm for nanostructured flat-foil with a nanosphere diameter of 40 nm.

Conclusion is that E_x has the same behavior in both methods when nanosphere diameters vary from 30 nm to 40 nm.

Chapter 5

"MATHEMATICAL DESCRIPTION OF THE DENSITY PROFILE FOR THE INTERACTION OF AN ULTRA-HIGH INTENSITY LASER PULSE WITH A NANOSTRUCTURED FLAT-TOP CONE"

We proposed a new cone target that has walls and top of the cone covered with nanospheres tangent to each other and tangent to the cone walls.

I will mathematically describe the density profile of the initial plasma created by an ultra-high intensity laser pulse that interacts this cone. This density profile is designed to be used in two-dimensional PIC codes for laser acceleration – ion.

In the first subchapter I describe the nanostructured flat cone inside a simulation box.

The nanostructured flat cone parameters are relative to a cartesian coordinate system whose origin O is the lower left corner of the simulation box. Ox and Oy axes are the two perpendicular sides of the simulation box that intersect at point O. The target has a conical shape with curved walls. Both walls have a given thickness, g_{wall}.

The walls are circular arcs of circles with R_1 and $R_2 = R_1 + g_{wall}$ rays, with centers $C_1(x_1, c_1)$ and $C_2(x_2, c_2 = l_y - c_1)$. At the top there is a foil with g_{foil} thickness and l_{foil}. length. Other parameters of the nanostructured cone are: h_{cone}, height, g_{base} ,large base of the cone and g_{neck} small base of the cone. All nanospheres have the same diameter d_{ns}. The nanostructured cone is inserted into a simulation box with a width l_x and a height l_y. . In PIC simulations it must be considered that we have a vacuum before the target. We note the width of the vacuum with l_v.

We noted $M(x_M, y_M)$ a mathematical point associated with a charged particle (electron, proton or ion) and noted the following known angles: θ, α, φ that I used in the formulas describes in this chapter.

In the second subchapter we obtained the formula of the number of nanospheres at the top of the cone and on the walls of the cone according to g_{neck} and d_{ns}, respectively according to θ, α, φ and we obtained the formulas:

$$m = \left[\frac{g_{neck}}{d_{ns}}\right], n = \left[\frac{\alpha - \theta}{\varphi}\right]$$

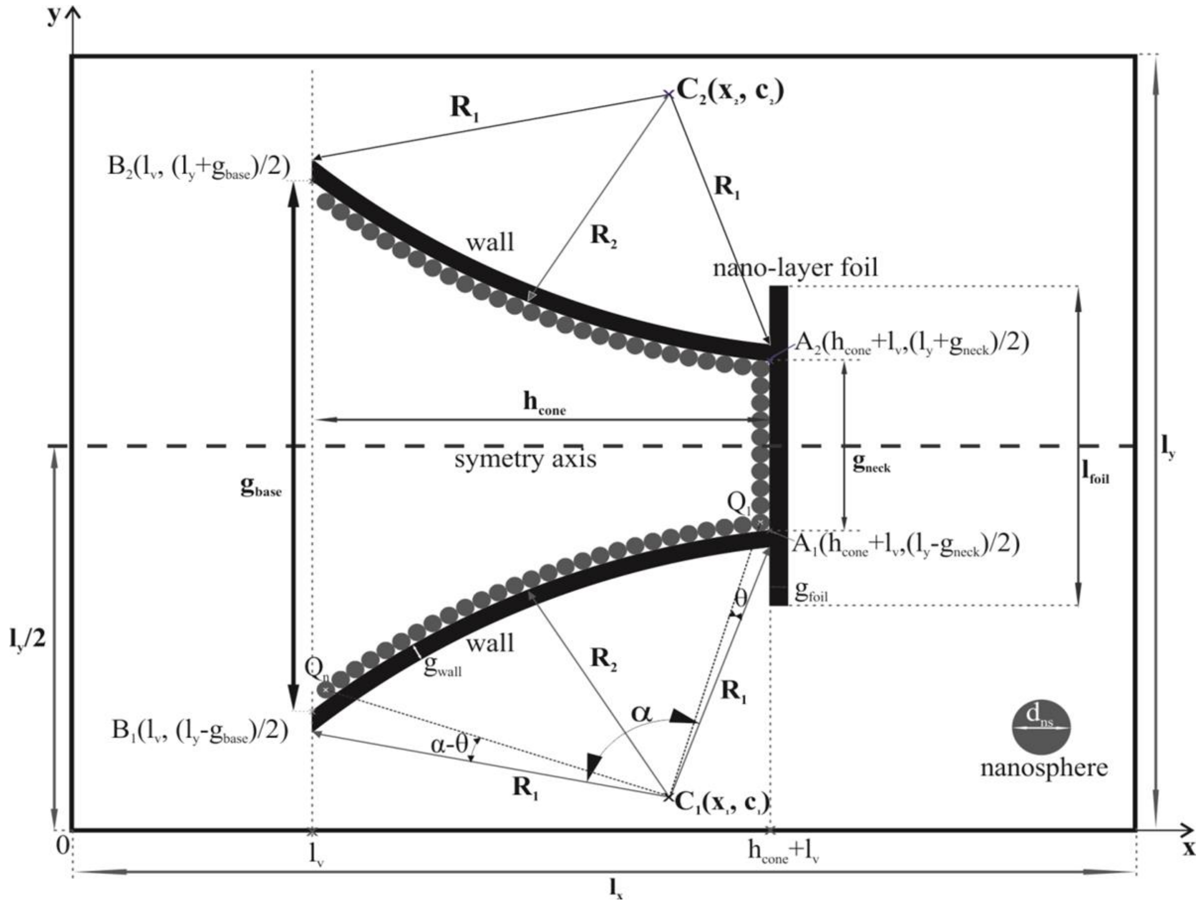

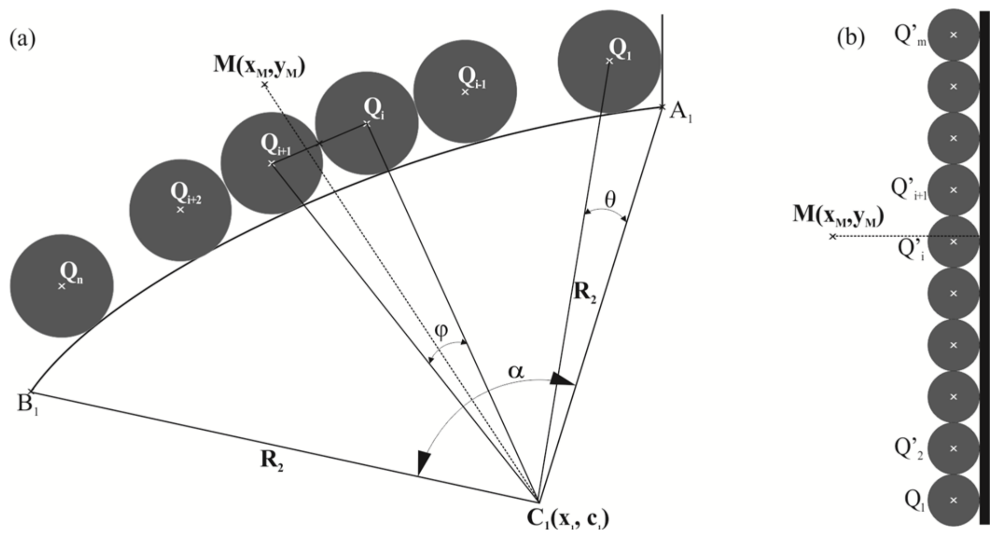

In the third subchapter we I found out the conditions that a particle loaded from the initial plasma must meet in order to be inside a nanosphere. We were able to determine the coordinates of the nanosphere centers according to the known parameters and thus, describe the algorithm to find out the position of a plasma particle according to the centers of the nanofers inside the conical target and the parameters defined at the beginning.

CONCLUSIONS

GENERAL CONCLUSIONS

In my doctoral thesis I addressed a topical topic regarding the acceleration of particles to the interaction of an ultra-high intensity laser pulsewith new solid targets, microcones and ultra-thin nanostructured flat-foil target, with thicknesses of the order of tens of nanometers. For these targets we used parameters similar to those of ELI-NP lasers, in case of acceleration of protons and carbon ions

From the results obtained for the interaction of the ultraintens laser pulse with the nanostructured flat-foil target we can conclude that in case of proton acceleration we have better results for the foils that have deposited a layer of nanospheres on them, the exception to this being in the case of accelerating carbon ions, where we have obtained that the dependence on the diameter of the nanosphere of the maximum energy of the carbon ions is very weak for both polarizations of the laser pulse.

ORIGINAL CONTRIBUTIONS

- Following my research done and presented in my doctoral dissertation, we have concluded that highest energies and a large number of carbon ions C^{6+} and very energetic protons are obtained in the case of nanosphere cone targets.
- We have obtained that the optimal target for which we have the maximum number of very energetic particles with low angular divergence:
  1) For carbon ions the target is cone with nanospheres with a nanosphere diameter of 80 nm and a nanostructured foil thickness of 40 nm;
  2) For protons the target is cone with nanospheres, for both linear and circular polarized laser pulse.

We compared the distribution of the electromagnetic field obtained by the FDTD method with that obtained with the PIC method and we have the same sudden decrease of E_x values from nanostructured foil with a nanosphere diameter of *30 nm* to a nanostructured foil with a nanosphere diameter of *40 nm.*

We determined analytical formulas that mathematically describe the density profile in the case of a conical target with nanosphere, which are then transposed into a simple mathematical algorithm.

SUBSEQUENT DEVELOPMENT PERSPECTIVES

This doctoral thesis creates important perspectives for the development and continuation of research in the field of particle acceleration following the interaction of an ultra-high intensity laser pulse with cone targets and flat foils:

- By using three-dimensional PIC simulations, following which more appropriate and conclusive results of the energies of accelerated protons and carbon ions can be obtained.
- By transposing into a calculation code the algorithm obtained to describe the density profile in the case of nanosphere cones.
- By using the results obtained which are intended to be used in future experiments from ELI-NP.